

Electronic Supplementary Information

Probing the Ligand Exchange Kinetics of Phenynyl-based Ligands on Colloidal Au Nanoparticles

Ting Xiang, Jianpeng Zong, Wenjia Xu, Yuhua Feng and Hongyu Chen**

Institute of Advanced Synthesis (IAS), School of Chemistry and Molecular Engineering, Jiangsu
National Synergetic Innovation Centre for Advanced Materials, Nanjing Tech University, Nanjing
211816, P. R. China.

Email: iashychen@njtech.edu.cn; ias_yhfeng@njtech.edu.cn

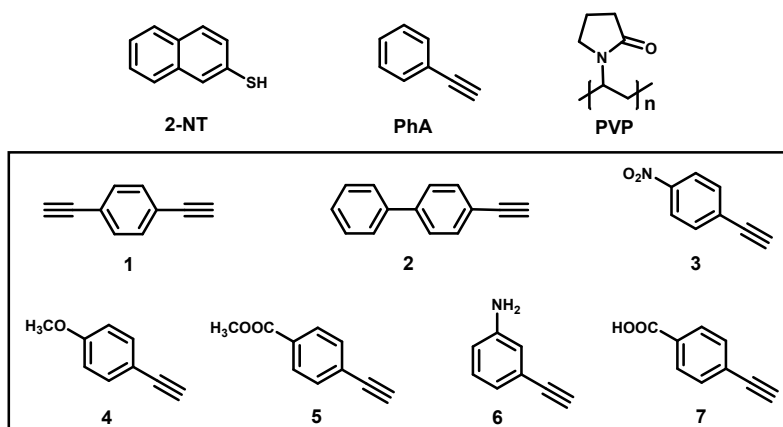


Figure S1. Ligands used in the study: 2-naphthalenethiol (2-NT); phenylacetylene (PhA); polyvinylpyrrolidone (PVP); 1, 1,4-diethynylbenzene; 2, 4-ethynyl-1,1'-biphenyl; 3, 4-nitrophenylacetylene; 4, 4-ethynylanisole; 5, 4-ethynyl-benzoic acid methyl ester; 6, 3-aminophenylacetylene; 7, 4-ethynyl-benzoic acid.

Chemicals

All chemicals were used as received without further purification. Hydrogen tetrachloroaurate (III) trihydrate (HAuCl_4 , 99.9%, Au 49% on metals basis, Alfa Aesar); sodium citrate tribasic dihydrate ($\text{NaC}_6\text{H}_5\text{O}_7 \cdot 2\text{H}_2\text{O}$, 99%, Alfa Aesar); sodium hydroxide (NaOH, 96%, Aladdin); 2-naphthalenethiol ($\text{C}_{10}\text{H}_8\text{S}$, 98%, Aldrich); polyvinylpyrrolidone (PVP, Mw = 40,000, Aldrich); phenylacetylene (C_8H_6 , 96%, Energy); 1,4-diethynylbenzene (C_{10}H_6 , 97%, J&K); 4-ethynyl-1,1'-biphenyl ($\text{C}_{14}\text{H}_{10}$, 98%, Energy); 4-nitrophenylacetylene ($\text{C}_8\text{H}_5\text{NO}_2$, 97%, J&K); 4-ethynylanisole ($\text{C}_9\text{H}_8\text{O}$, 98%, Macklin); 4-ethynyl-benzoic acid methyl ester ($\text{C}_{10}\text{H}_8\text{O}_2$, 97%, Aladdin); 3-aminophenylacetylene ($\text{C}_8\text{H}_7\text{N}$, 99%, J&K); 4-ethynyl-benzoic acid ($\text{C}_9\text{H}_6\text{O}_2$, 96%, Adamas); N,N-dimethylformamide (DMF, 99.9%, J&K); deionized water (resistance $> 18.2 \text{ M}\Omega \cdot \text{cm}^{-1}$).

Characterizations

Absorption spectra were collected on a Cary 100 UV-Vis spectrophotometer (VARIAN). TEM images were collected by using Transmission Electron Microscopy operated at 120 kV (FEI-Talos L120C). Raman and SERS spectra were collected from the as-synthesized sample solutions in a quartz cuvette (pathlength = 1.00 cm) on a portable Raman analyzer (Accuman SR-510 Pro) equipped with 785 nm red LED laser. The laser power is 350 mW and the integration time is 3 s.

XPS spectra were collected on Thermo Fisher Scientific X-ray photoelectron spectrometer (K-ALPHA+).

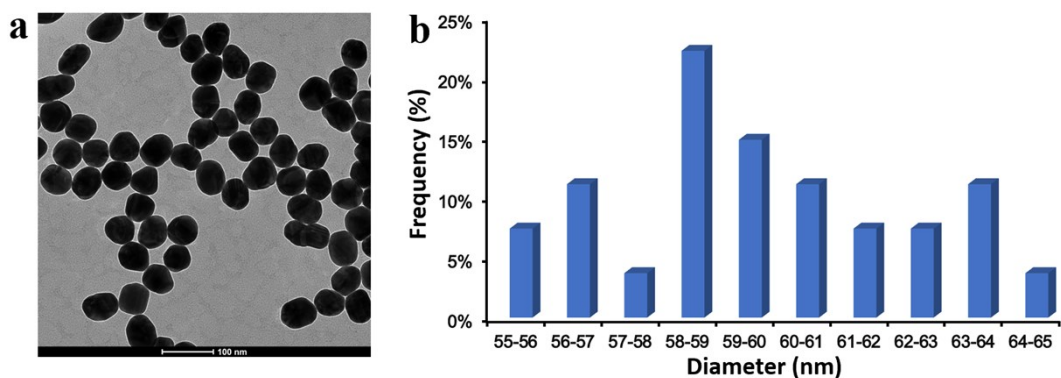


Figure S2. (a) TEM image of the as-synthesized 60 nm AuNPs; (b) the size distribution of the AuNPs.

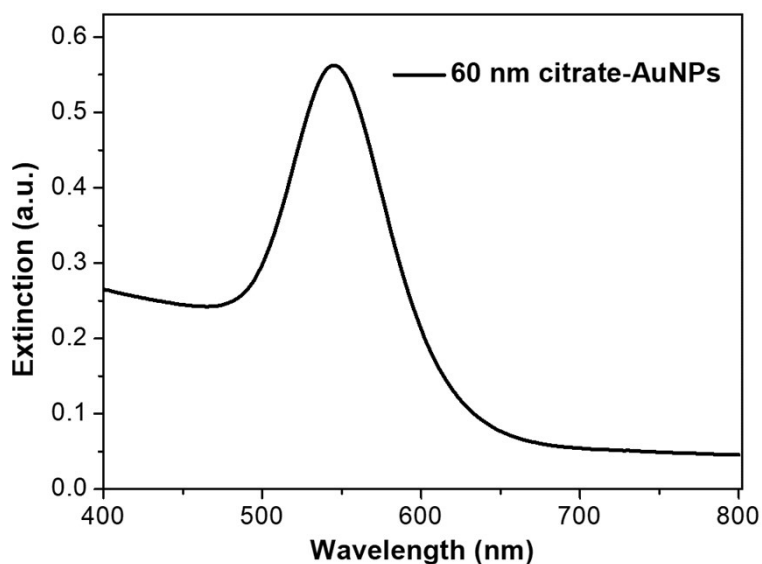


Figure S3. UV-vis spectra of 60 nm citrate-AuNPs.

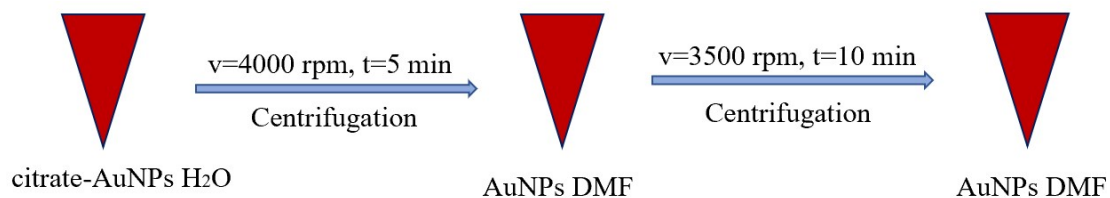


Figure S4. Schematics illustrating the phase transfer of 60 nm citrate-AuNPs from water to DMF.

The calculation of SERS enhancement factor:

The 1588 cm^{-1} Raman peak of PhA, whose intensity is the strongest in both Raman and SERS spectra, was used to calculate the SERS enhancement factor of PhA-AuNPs. The calculation is based on the following equation:

$$EF = (I_{\text{SERS}} \times C_{\text{bulk}}) / (I_{\text{bulk}} \times C_{\text{SERS}})$$

Where I_{SERS} and I_{bulk} are the Raman intensities of the same 1588 cm^{-1} peak for PhA-AuNPs and PhA in DMF solution, C_{SERS} and C_{bulk} are the concentrations of PhA on AuNPs (PhA-AuNPs) and PhA in DMF solution.

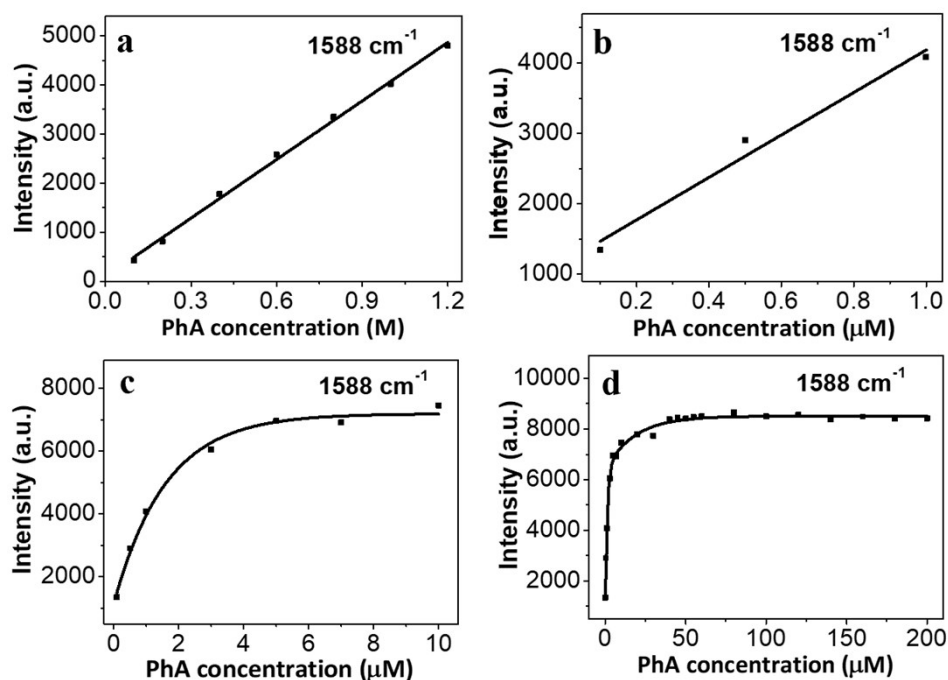


Figure S5. (a) Plot and linear fit of Raman intensity vs PhA concentration in DMF (0~1.2 M) for 1588 cm^{-1} Raman peak. SERS intensity of (b) 0.1~1 μM , (c) 0.1~10 μM , (d) 0.1~200 μM PhA-AuNPs in DMF.

We find that the PhA concentration (0.2 M) is near the linear fit, the corresponding SERS intensity is 913, and the SERS intensity of PhA (1 μM) is 4081, the EF is 8.9×10^5 .

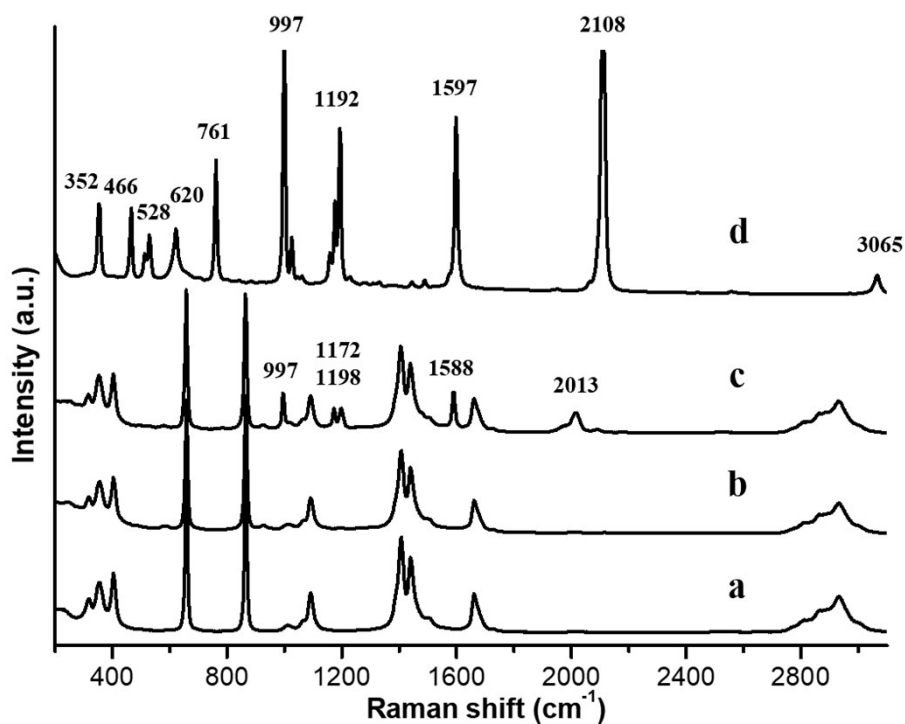


Figure S6 (a) Raman spectra of pure DMF. (b) SERS intensity of 60 nm citrate-AuNPs in DMF. (c) SERS intensity of 8.3 μ M PhA-AuNPs in DMF. (d) Raman spectra of pure PhA.

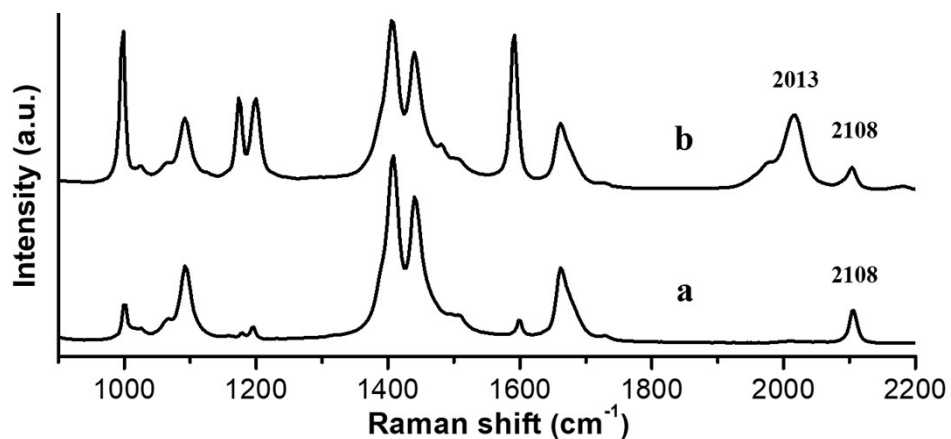


Figure S7. (a) Raman spectra of 200 mM pure PhA in DMF. (b) SERS intensity of 200 mM PhA-AuNPs in DMF.

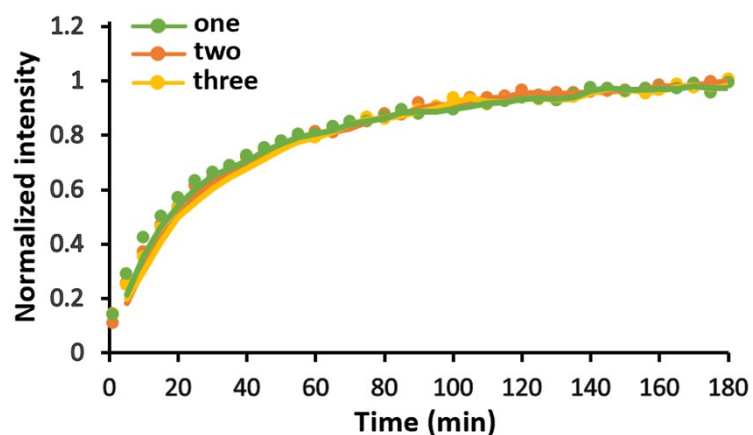


Figure S8. Normalized traces of SERS intensity at 2013 cm^{-1} during the incubation of citrate-AuNPs with $8.3\text{ }\mu\text{M}$ PhA in DMF for the same three samples.

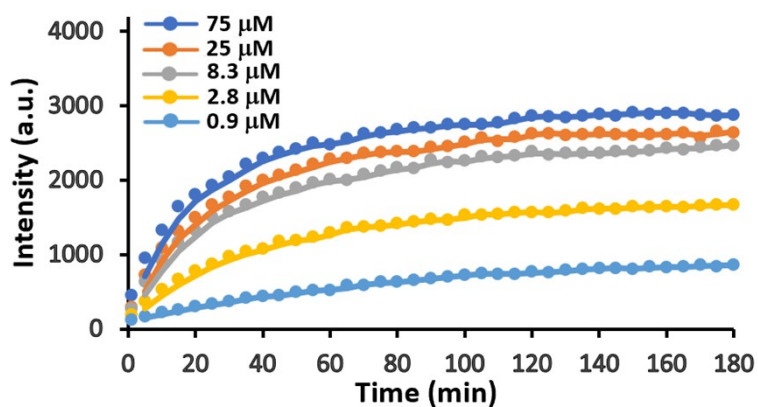


Figure S9. Normalized traces of SERS intensity at 2013 cm^{-1} during the incubation of citrate-AuNPs with PhA in DMF for the different concentration samples.

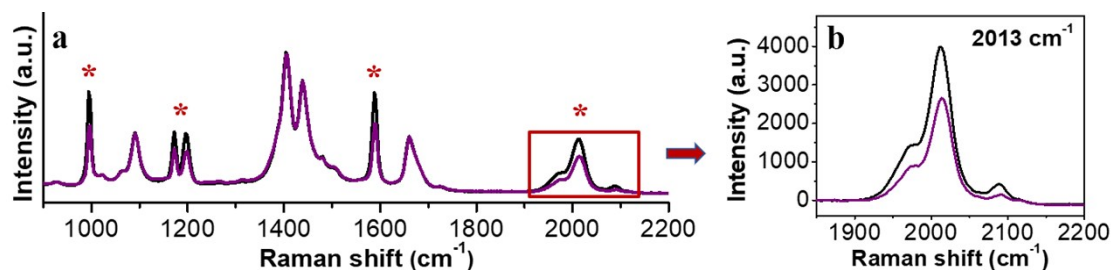


Figure S10. (a) SERS intensity of citrate-AuNPs after 3 h incubation with $8.3\text{ }\mu\text{M}$ PhA ligand without (black) and with (purple) Ar gas bubbling. (b) Expansion of the framed region in a.

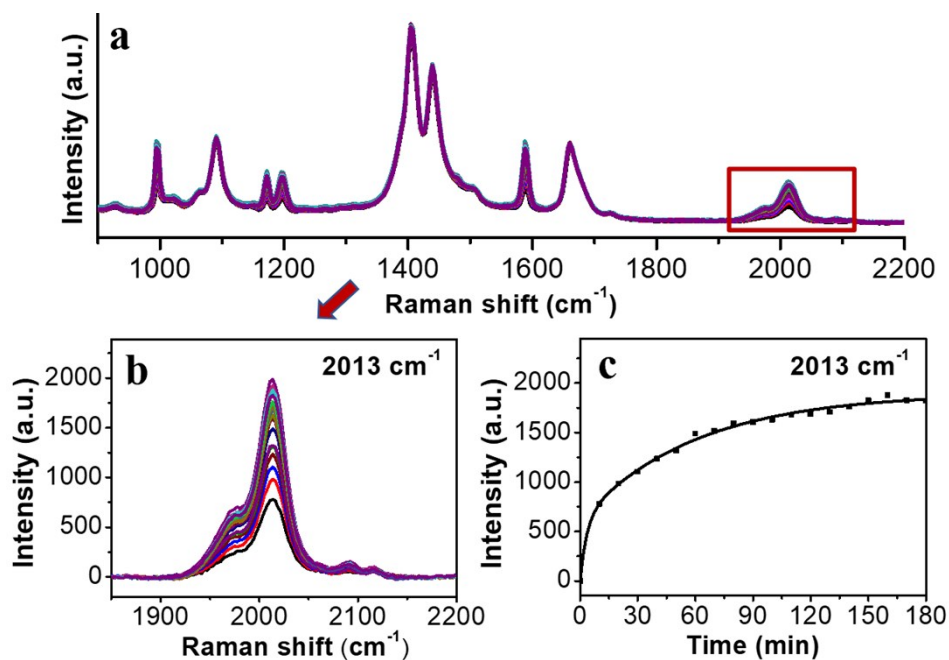


Figure S11. (a) Temporal evolution of the SERS intensity of citrate-AuNPs incubated with 8.3 μM PhA under Ar atmosphere in a cuvette which was sealed in a glove box. (b) Expansion of the framed region in a. (c) Intensity traces of the peak in b.

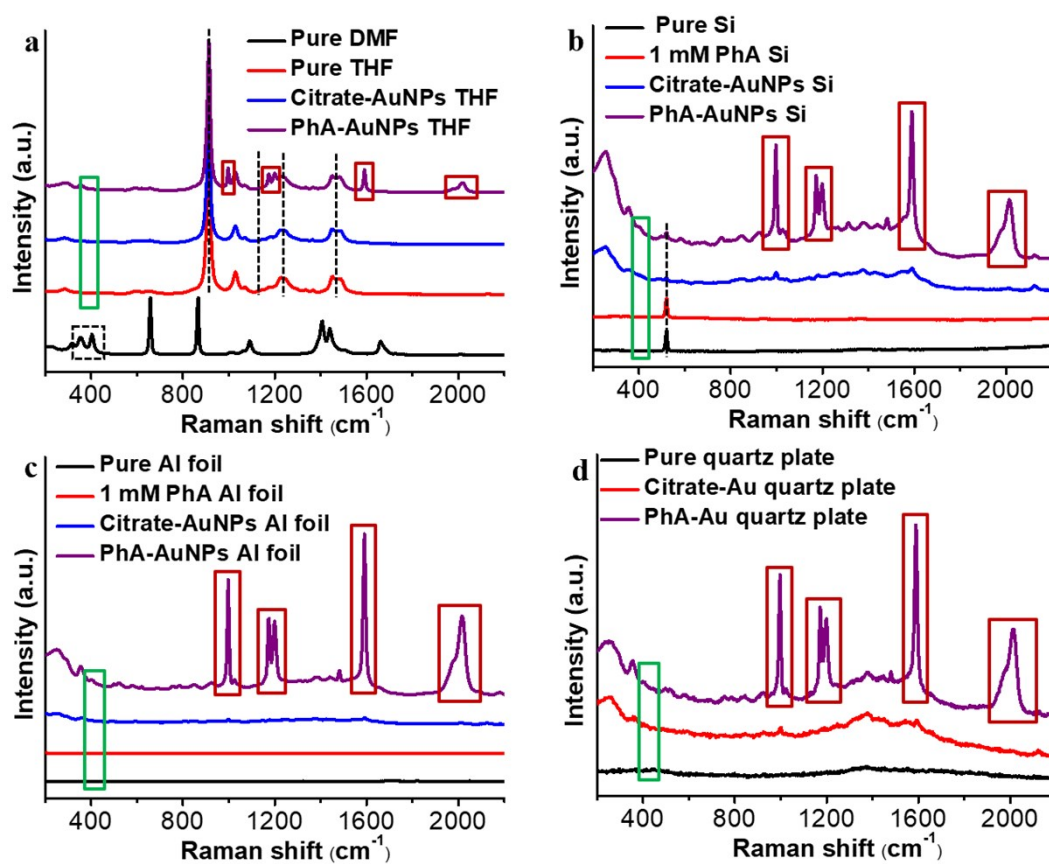


Figure S12. (a) Raman spectra of pure DMF (black), pure THF (red); SERS intensity of 60 nm

citrate-AuNPs (blue), PhA-AuNPs (purple) in THF. (b) Raman spectra of pure Si (black), 1 mM PhA (red) on Si; SERS intensity of 60 nm citrate-AuNPs (blue), PhA-AuNPs (purple) on Si. (c) Raman spectra of pure Al foil (black), 1 mM PhA (red) on Al foil; SERS intensity of 60 nm citrate-AuNPs (blue), PhA-AuNPs on Al foil. (d) Raman spectra of pure quartz plate (black); SERS intensity of 60 nm citrate-AuNPs (red), PhA-AuNPs (purple) on quartz plate.

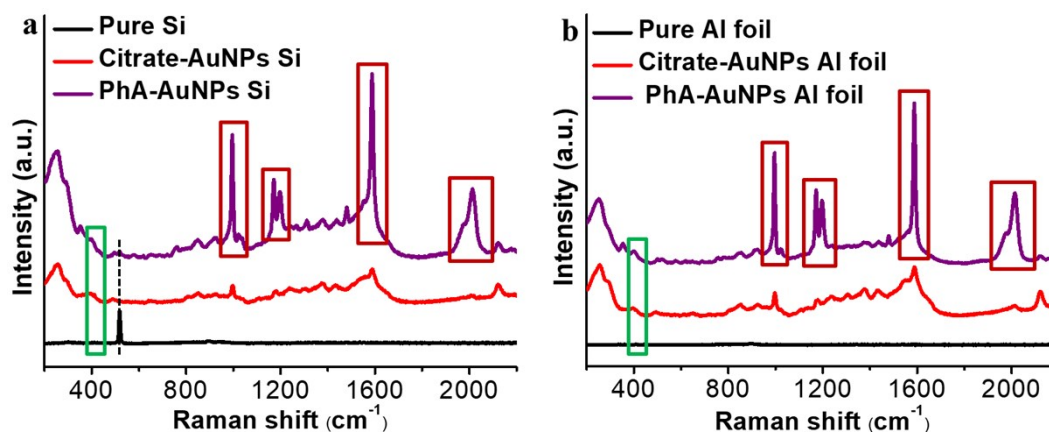


Figure S13. (a) Raman spectra of pure Si (black); SERS intensity of 60 nm citrate-AuNPs (red), PhA-AuNPs (purple) on Si. (b) Raman spectra of pure Al foil (black); SERS intensity of 60 nm citrate-AuNPs (red), PhA-AuNPs on Al foil.

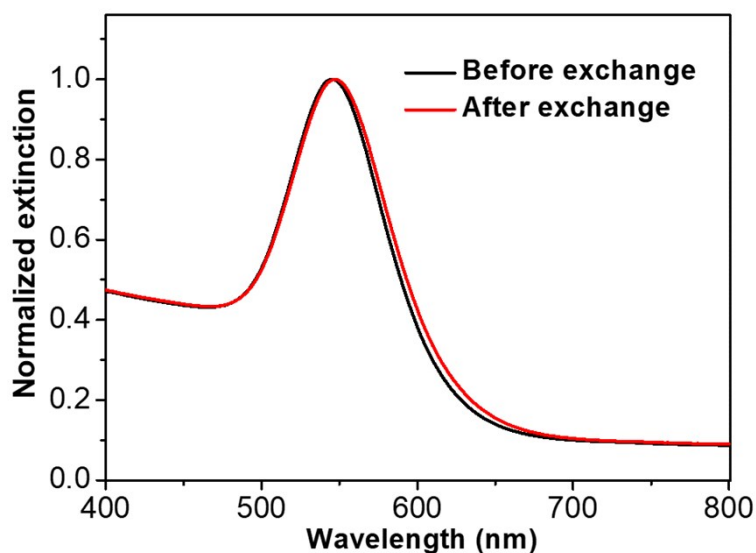


Figure S14. UV-vis spectra of AuNPs in DMF before and after 2-NT exchange PhA.

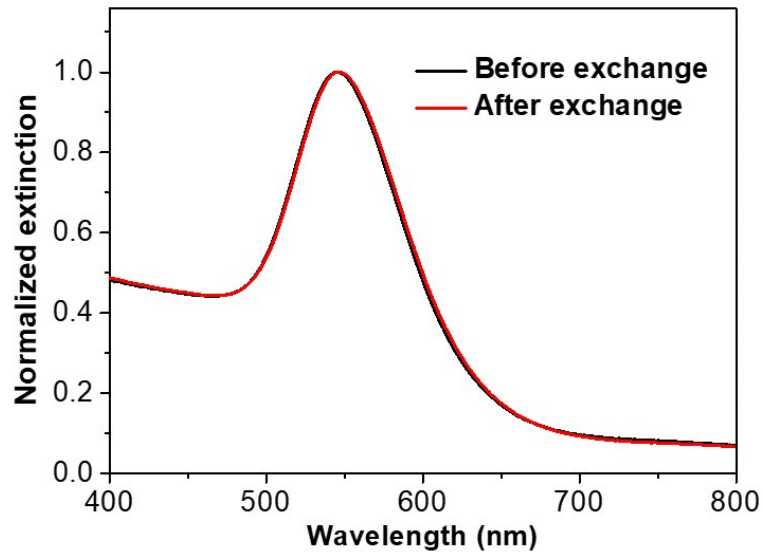


Figure S15. UV-vis spectra of AuNPs in DMF before and after PhA exchange 2-NT.

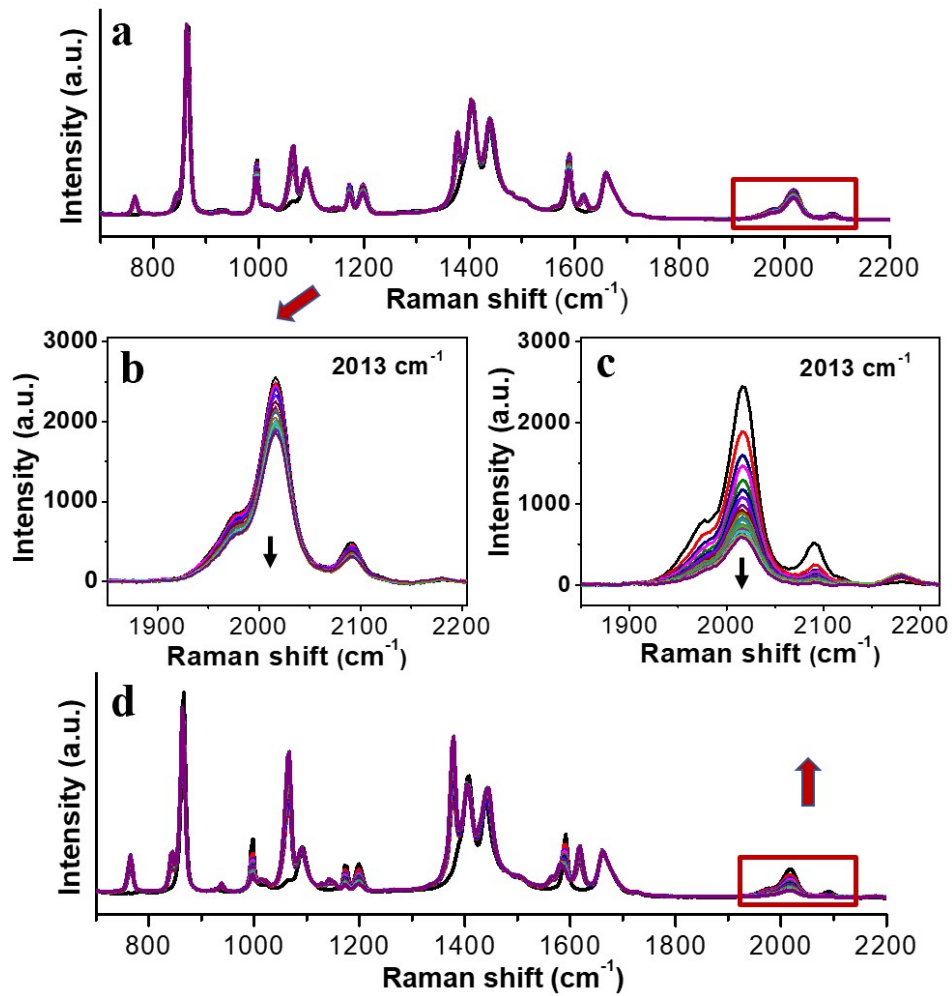


Figure S16. (a) Temporal evolution of the SERS intensity of 8.3 μM PhA-AuNPs incubated with 8.2 μM 2-NT in DMF at room temperature. (b) Expansion of the framed region in a. (c)

Expansion of the framed region in d. (d) Temporal evolution of the SERS intensity of $8.3 \mu\text{M}$ PhA-AuNPs incubated with $8.2 \mu\text{M}$ 2-NT in DMF at 60°C .

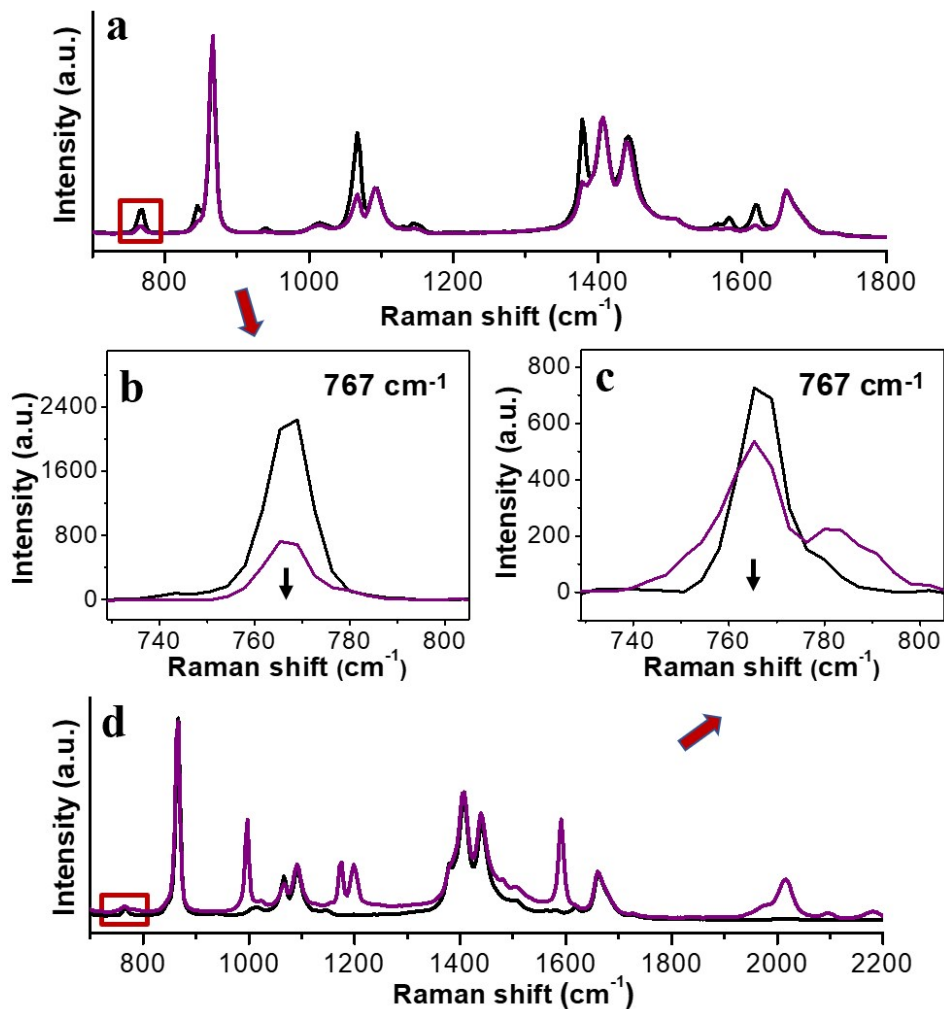


Figure S17. (a) The SERS intensity reduction 20 times of citrate-AuNPs incubated with 2-NT in DMF. (b) Expansion of the framed region in a. (c) Expansion of the framed region in d. (d) The SERS intensity of $0.41 \mu\text{M}$ 2-NT-AuNPs incubated with 20 mM PhA in DMF.

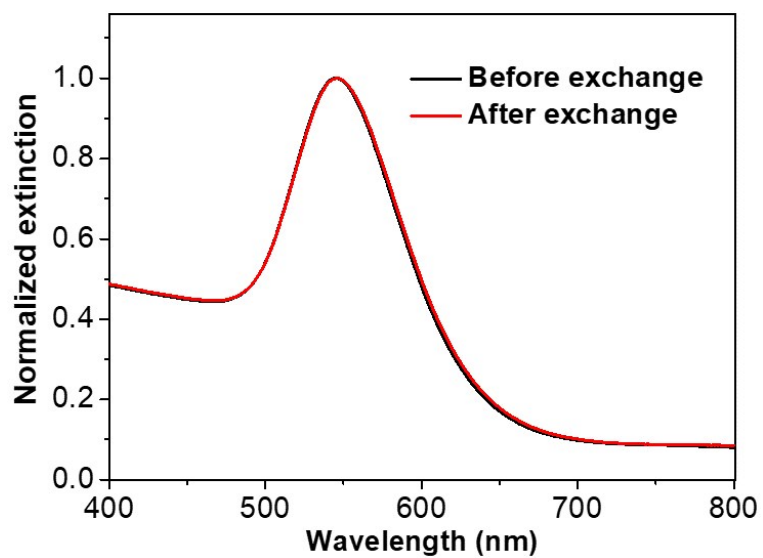


Figure S18. UV-vis spectra of AuNPs in DMF before and after PVP exchange PhA.

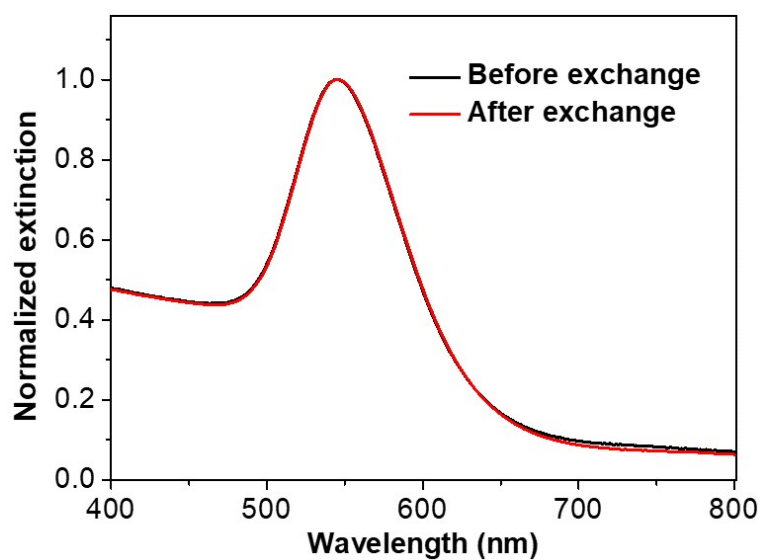


Figure S19. UV-vis spectra of AuNPs in DMF before and after PhA exchange PVP.

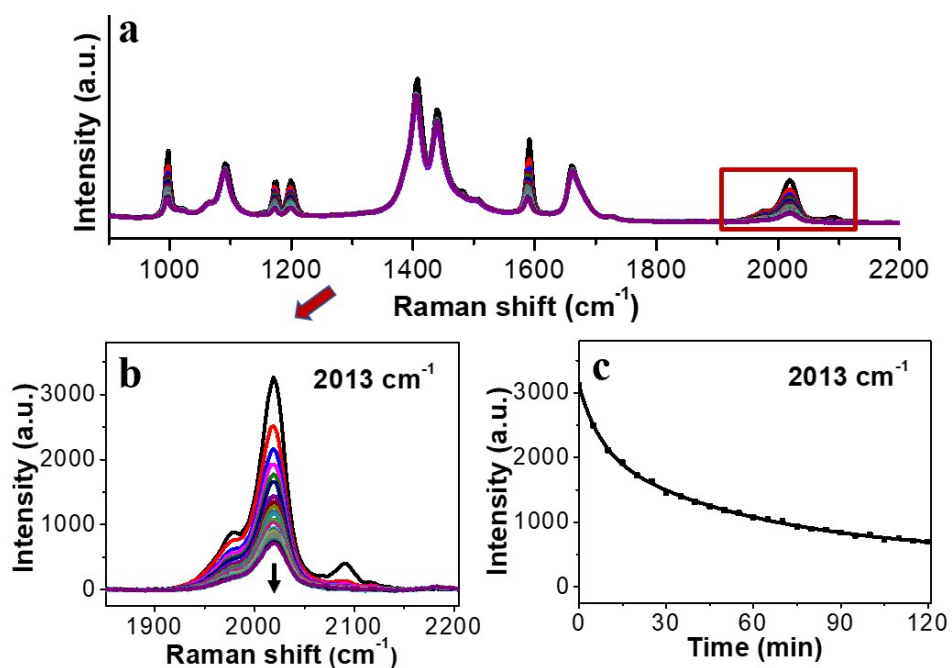


Figure S20. (a) Temporal evolution of the SERS intensity of 8.3 μM PhA-AuNPs incubated with 2.5 mM PVP in DMF. (b) Expansion of the framed region in a. (c) Intensity traces of the peak in b.

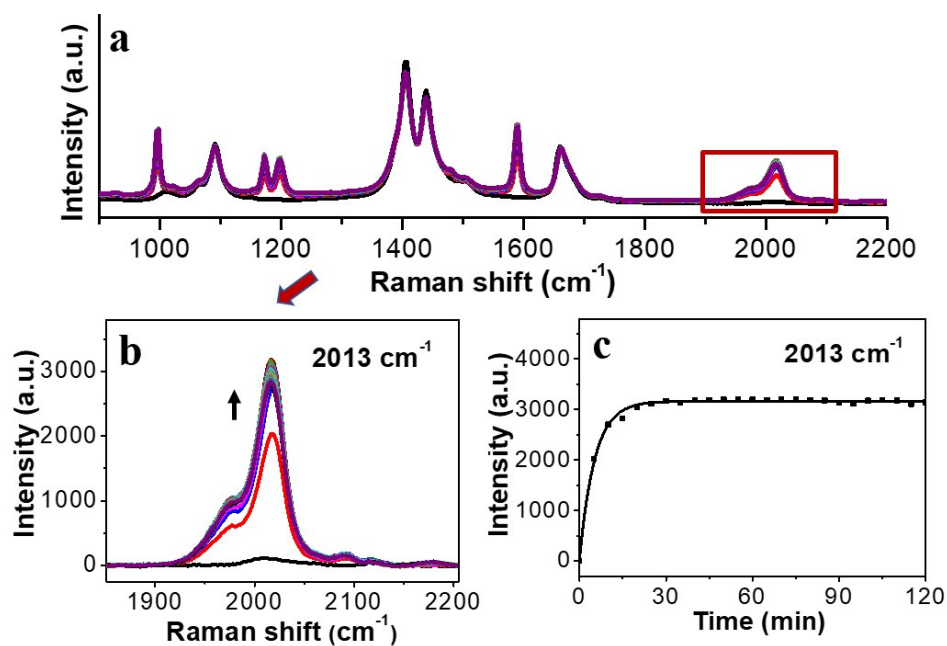


Figure S21. (a) Temporal evolution of the SERS intensity of 8.3 μM PVP-AuNPs incubated with 8.2 μM PhA in DMF. (b) Expansion of the framed region in a. (c) Intensity traces of the peak in b.

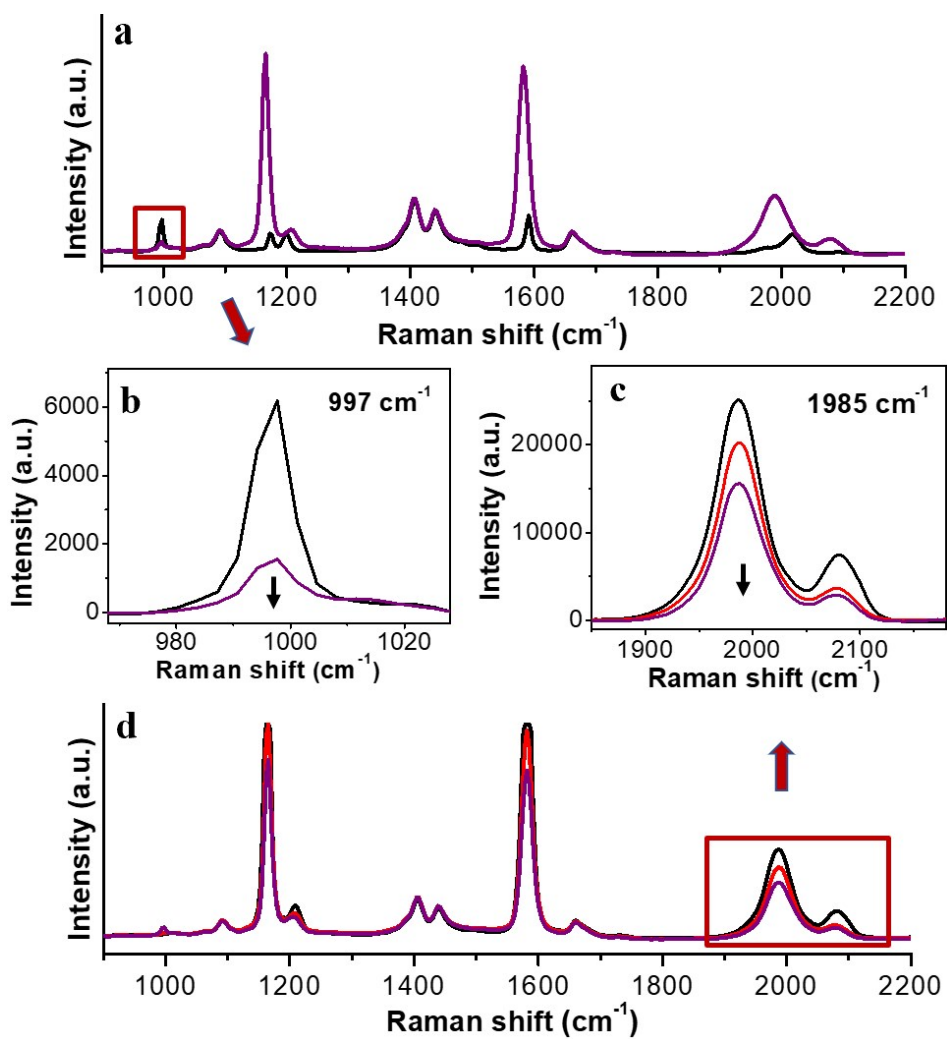


Figure S22. (a) Temporal evolution of the SERS intensity of 8.3 μM PhA-AuNPs incubated with 8.2 μM 1 in DMF. (b) Expansion of the framed region in a. (c) Expansion of the framed region in d. (d) Temporal evolution of the SERS intensity of 8.3 μM 1-AuNPs incubated with 8.2 μM (red) and 82 μM (purple) PhA in DMF.

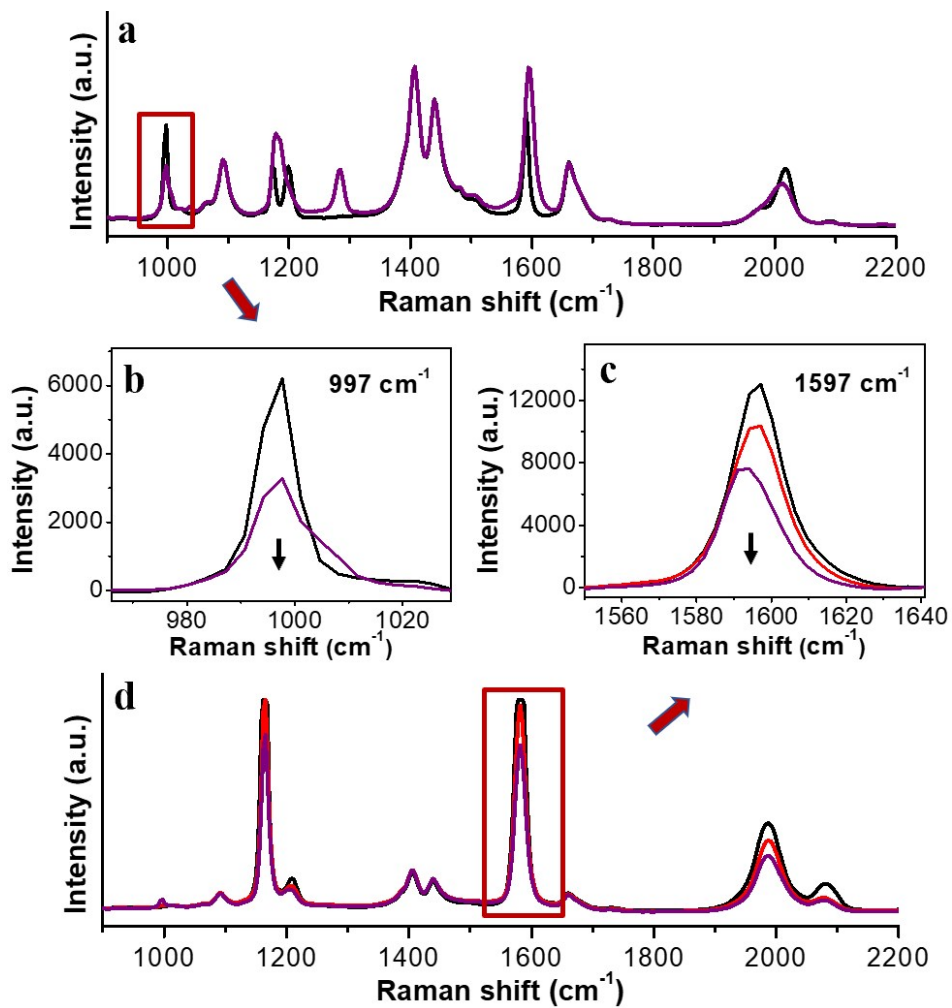


Figure S23. (a) Temporal evolution of the SERS intensity of 8.3 μM PhA-AuNPs incubated with 8.2 μM 2 in DMF. (b) Expansion of the framed region in a. (c) Expansion of the framed region in d. (d) Temporal evolution of the SERS intensity of 8.3 μM 2-AuNPs incubated with 8.2 μM (red) and 82 μM (purple) PhA in DMF.

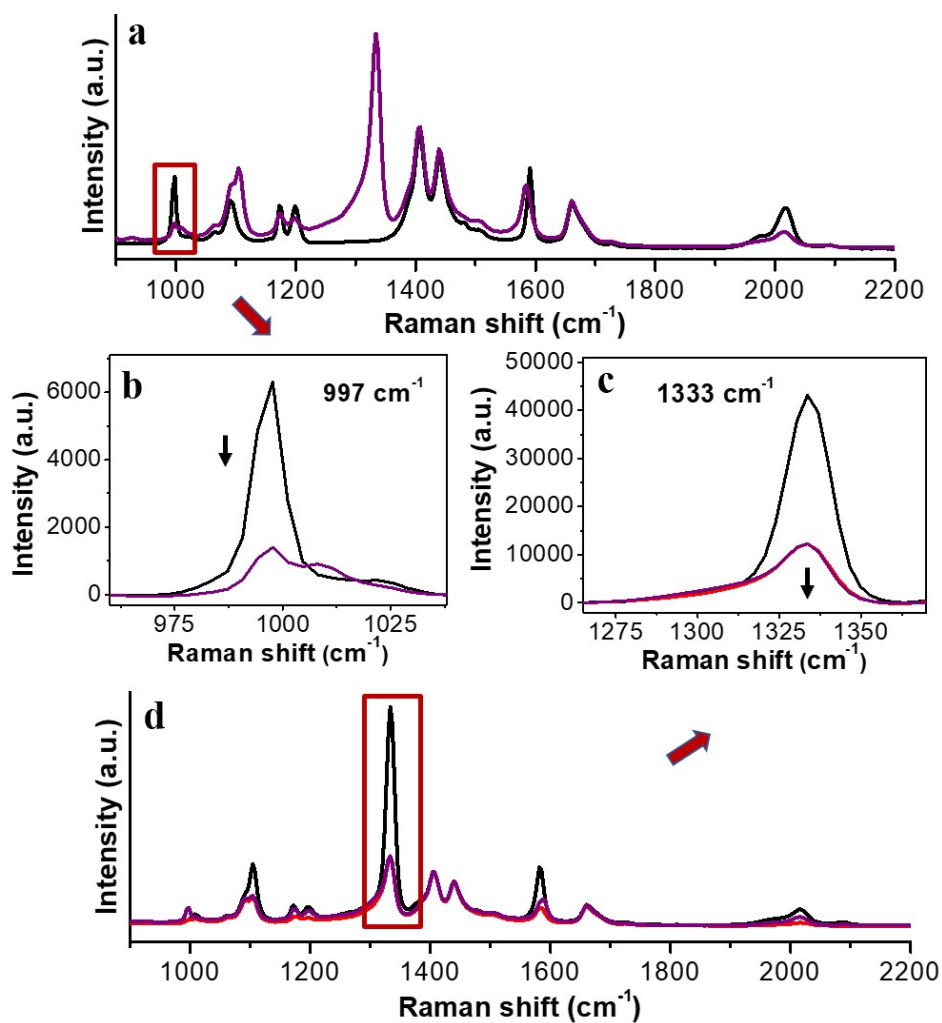


Figure S24. (a) Temporal evolution of the SERS intensity of 8.3 μM PhA-AuNPs incubated with 8.2 μM 3 in DMF. (b) Expansion of the framed region in a. (c) Expansion of the framed region in d. (d) Temporal evolution of the SERS intensity of 8.3 μM 3-AuNPs incubated with 8.2 μM (red) and 82 μM (purple) PhA in DMF.

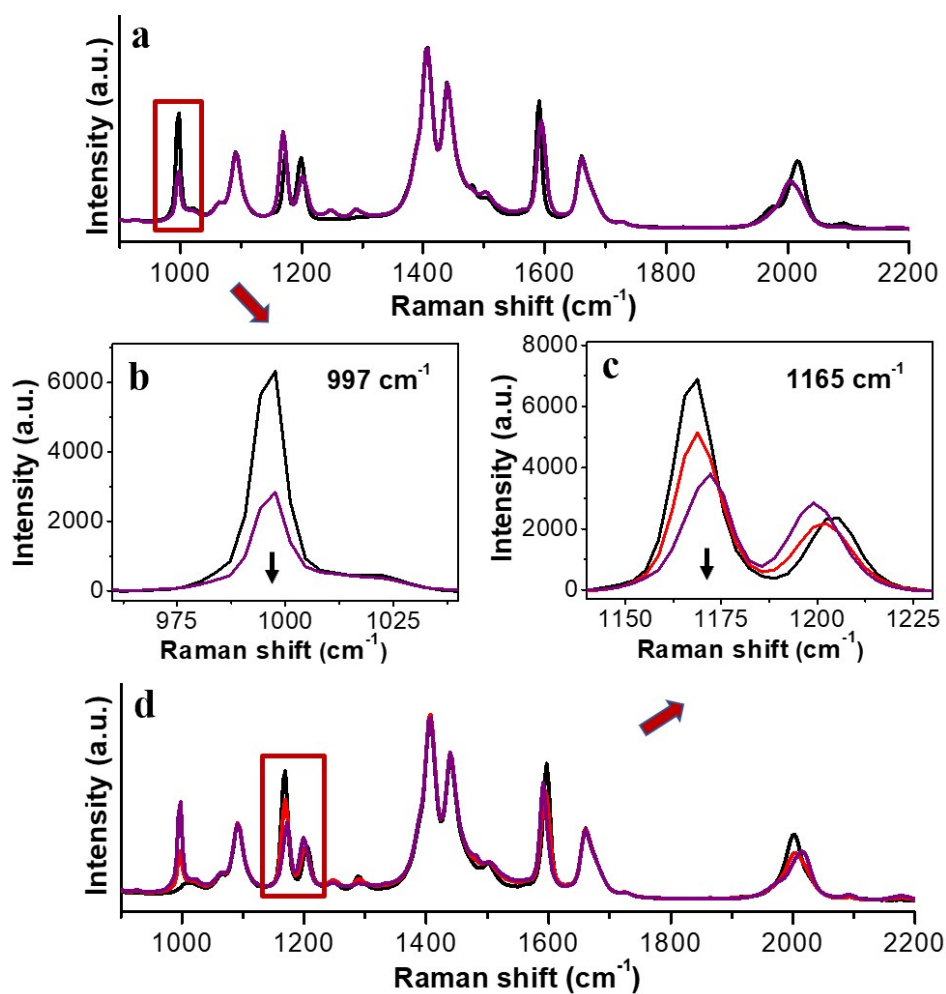


Figure S25. (a) Temporal evolution of the SERS intensity of 8.3 μM PhA-AuNPs incubated with 8.2 μM 4 in DMF. (b) Expansion of the framed region in a. (c) Expansion of the framed region in d. (d) Temporal evolution of the SERS intensity of 8.3 μM 4-AuNPs incubated with 8.2 μM (red) and 82 μM (purple) PhA in DMF.

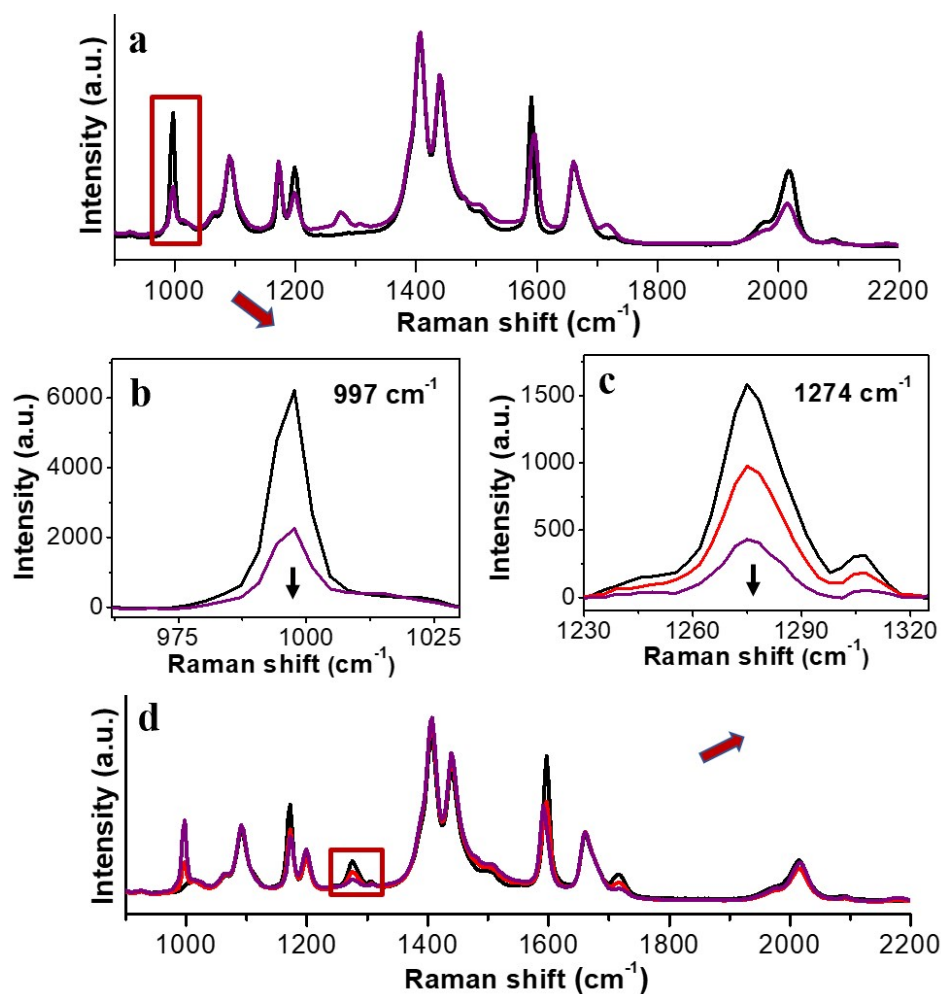


Figure S26. (a) Temporal evolution of the SERS intensity of 8.3 μM PhA-AuNPs incubated with 8.2 μM 5 in DMF. (b) Expansion of the framed region in a. (c) Expansion of the framed region in d. (d) Temporal evolution of the SERS intensity of 8.3 μM 5-AuNPs incubated with 8.2 μM (red) and 82 μM (purple) PhA in DMF.

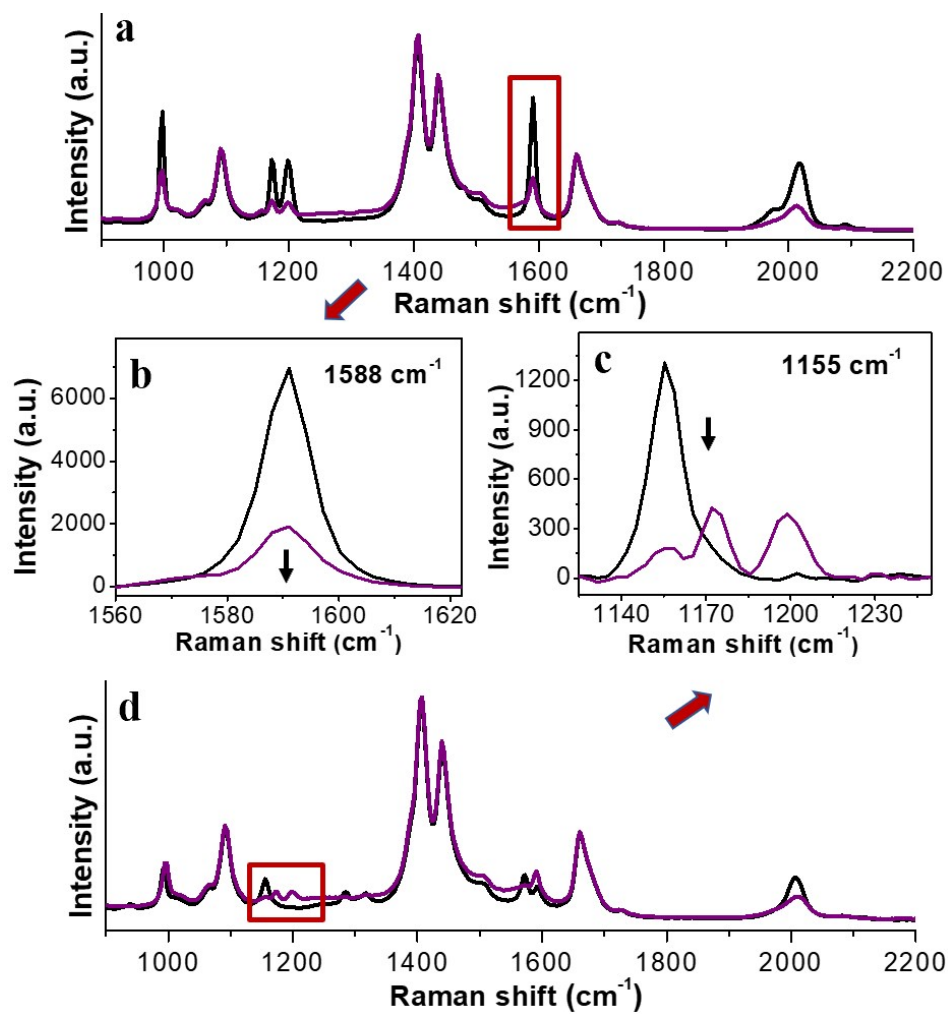


Figure S27. (a) Temporal evolution of the SERS intensity of 8.3 μM PhA-AuNPs incubated with 8.2 μM 6 in DMF. (b) Expansion of the framed region in a. (c) Expansion of the framed region in d. (d) Temporal evolution of the SERS intensity of 8.3 μM 6-AuNPs incubated with 8.2 μM PhA in DMF.

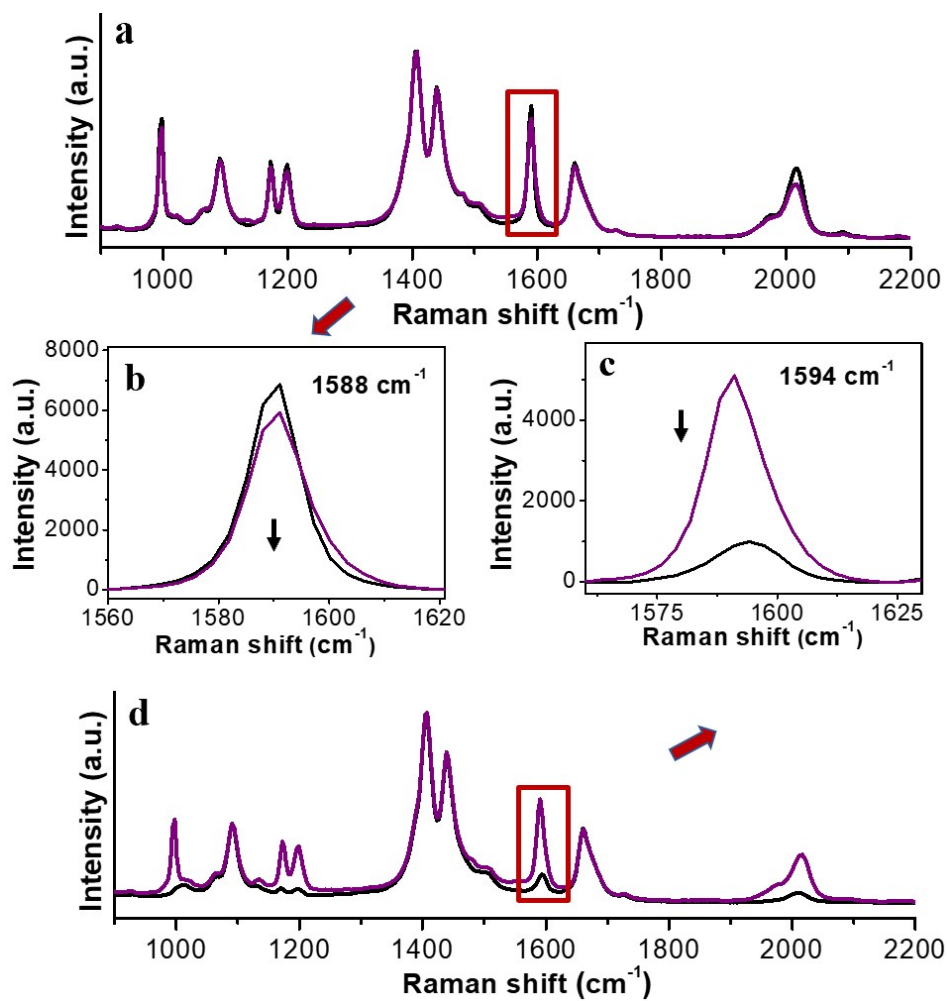


Figure S28. (a) Temporal evolution of the SERS intensity of 8.3 μM PhA-AuNPs incubated with 8.2 μM 7 in DMF. (b) Expansion of the framed region in a. (c) Expansion of the framed region in d. (d) Temporal evolution of the SERS intensity of 8.3 μM 7-AuNPs incubated with 8.2 μM PhA in DMF.

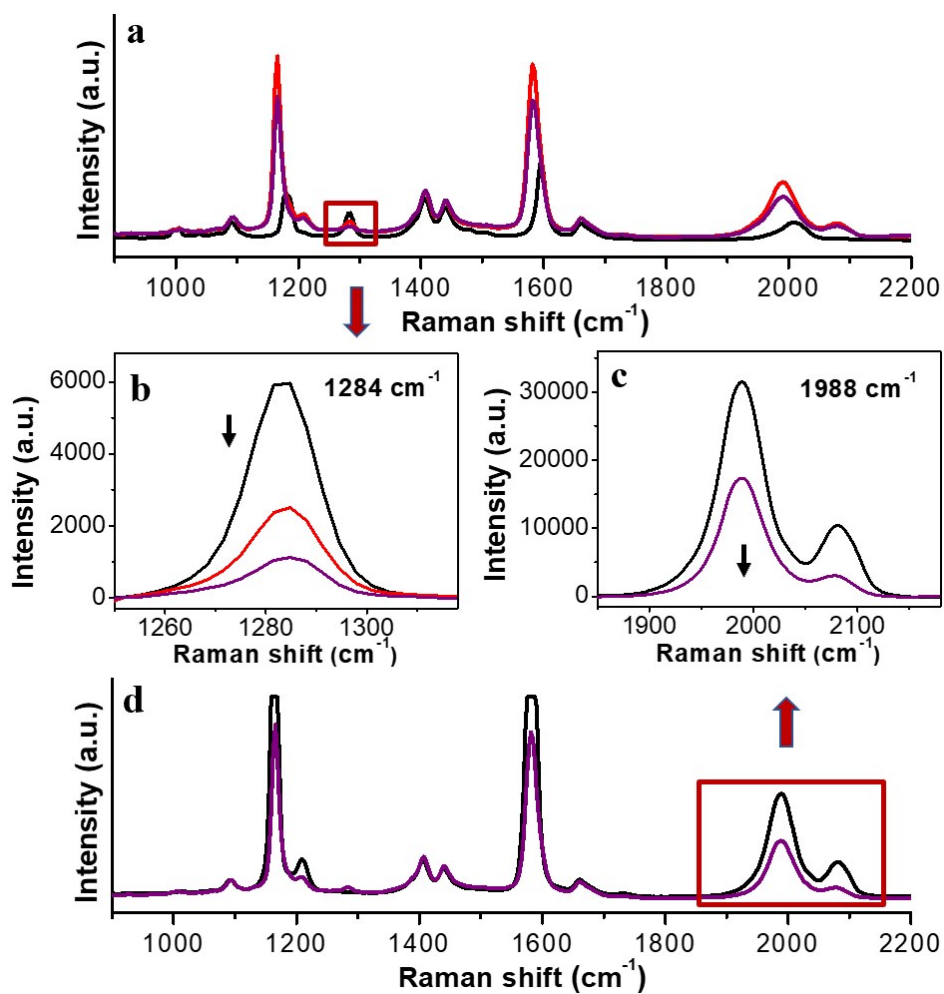


Figure S29. (a) Temporal evolution of the SERS intensity of 8.3 μM 2-AuNPs incubated with 8.2 μM (red) and 82 μM (purple) 1 in DMF. (b) Expansion of the framed region in a. (c) Expansion of the framed region in d. (d) Temporal evolution of the SERS intensity of 8.3 μM 1-AuNPs incubated with 82 μM 2 in DMF.

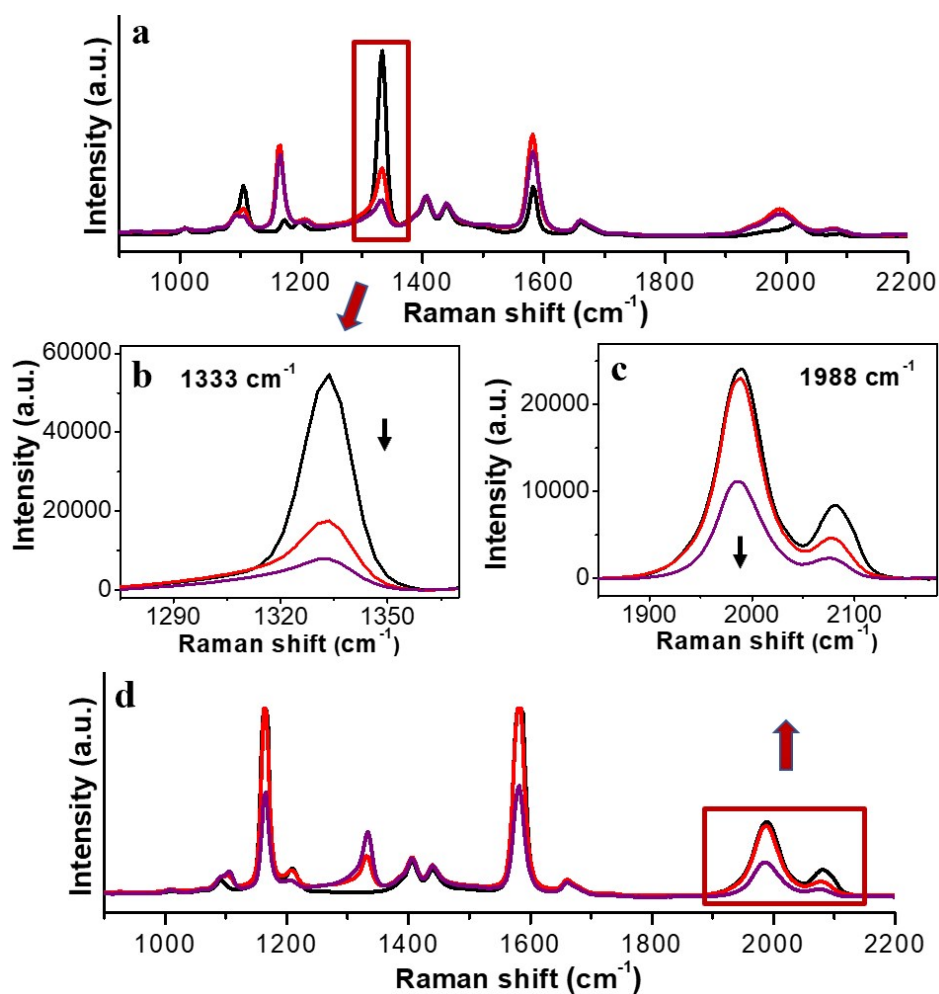


Figure S30. (a) Temporal evolution of the SERS intensity of 8.3 μM 3-AuNPs incubated with 8.2 μM (red) and 82 μM (purple) 1 in DMF. (b) Expansion of the framed region in a. (c) Expansion of the framed region in d. (d) Temporal evolution of the SERS intensity of 8.3 μM 1-AuNPs incubated with 8.2 μM (red) and 82 μM (purple) 3 in DMF.

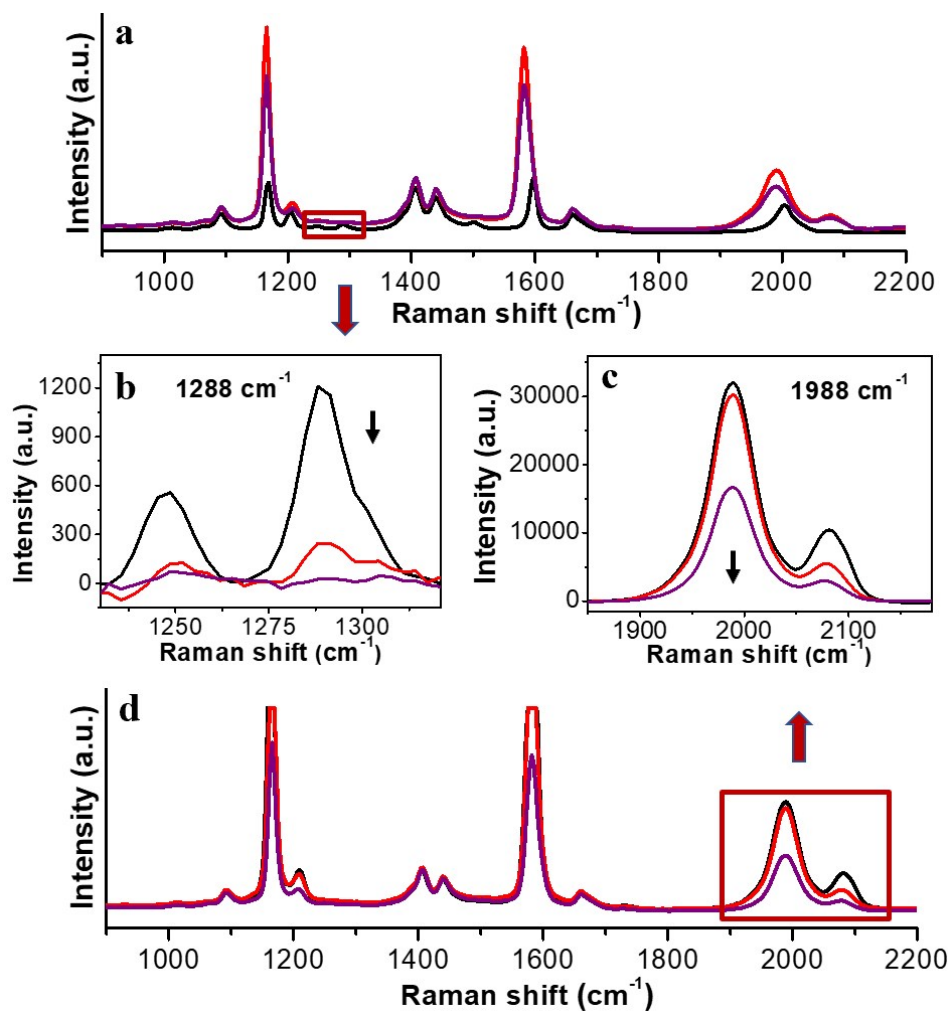


Figure S31. (a) Temporal evolution of the SERS intensity of $8.3 \mu\text{M}$ 4-AuNPs incubated with $8.2 \mu\text{M}$ (red) and $82 \mu\text{M}$ (purple) 1 in DMF. (b) Expansion of the framed region in a. (c) Expansion of the framed region in d. (d) Temporal evolution of the SERS intensity of $8.3 \mu\text{M}$ 1-AuNPs incubated with $8.2 \mu\text{M}$ (red) and $82 \mu\text{M}$ (purple) 4 in DMF.

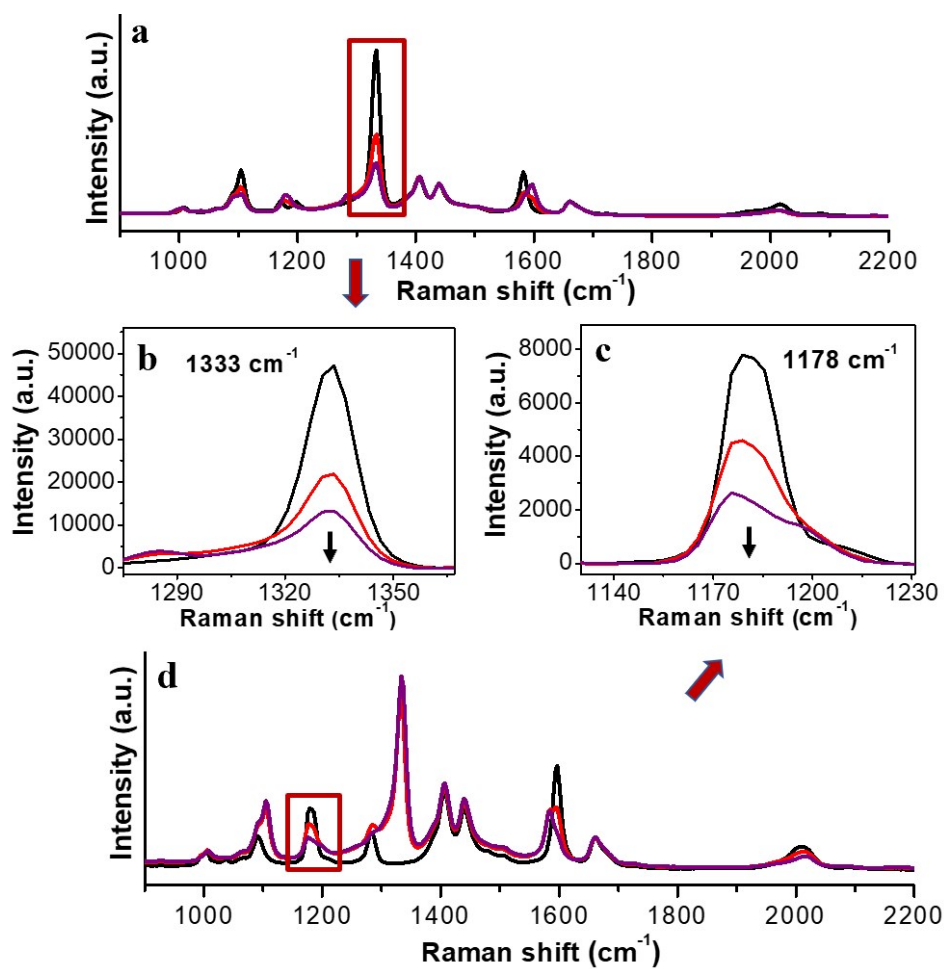


Figure S32. (a) Temporal evolution of the SERS intensity of 8.3 μM 3-AuNPs incubated with 8.2 μM (red) and 82 μM (purple) 2 in DMF. (b) Expansion of the framed region in a. (c) Expansion of the framed region in d. (b) Temporal evolution of the SERS intensity of 8.3 μM 2-AuNPs incubated with 8.2 μM (red) and 82 μM (purple) 3 in DMF.

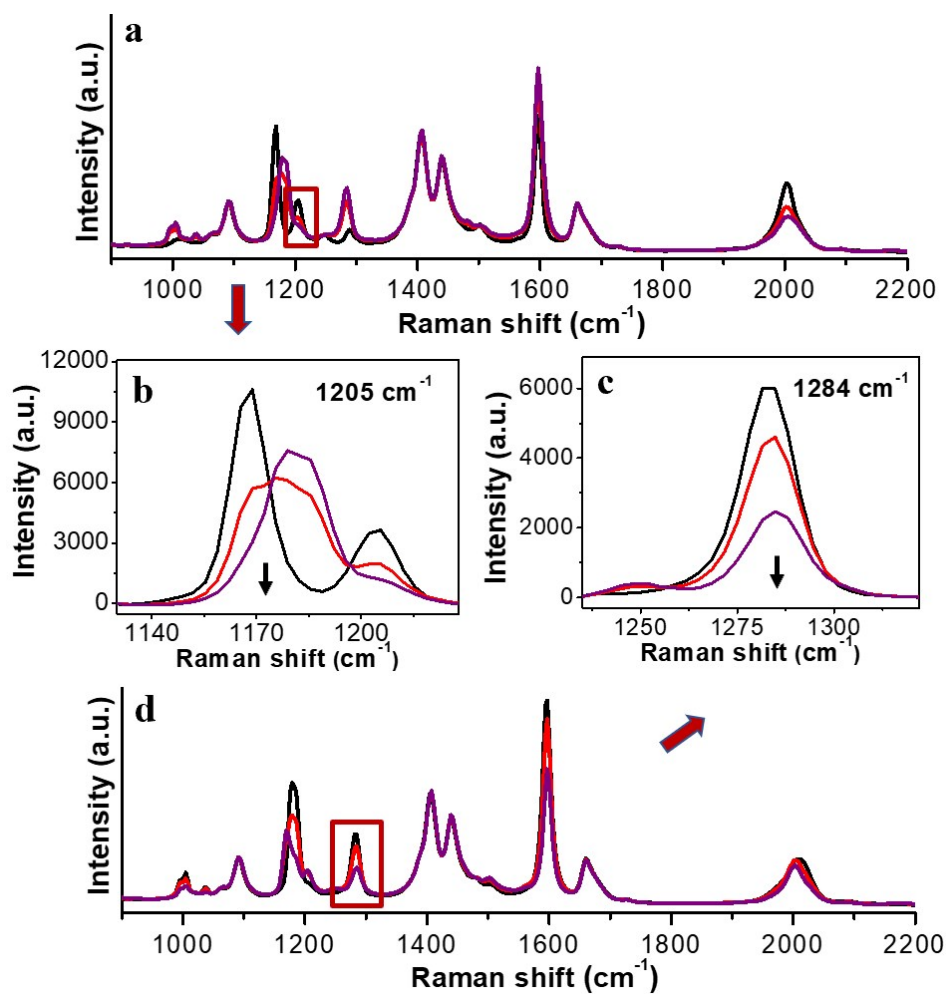


Figure S33. (a) Temporal evolution of the SERS intensity of 8.3 μM 4-AuNPs incubated with 8.2 μM (red) and 82 μM (purple) 2 in DMF. (b) Expansion of the framed region in a. (c) Expansion of the framed region in d. (c) Temporal evolution of the SERS intensity of 8.3 μM 2-AuNPs incubated with 8.2 μM (red) and 82 μM (purple) 4 in DMF.

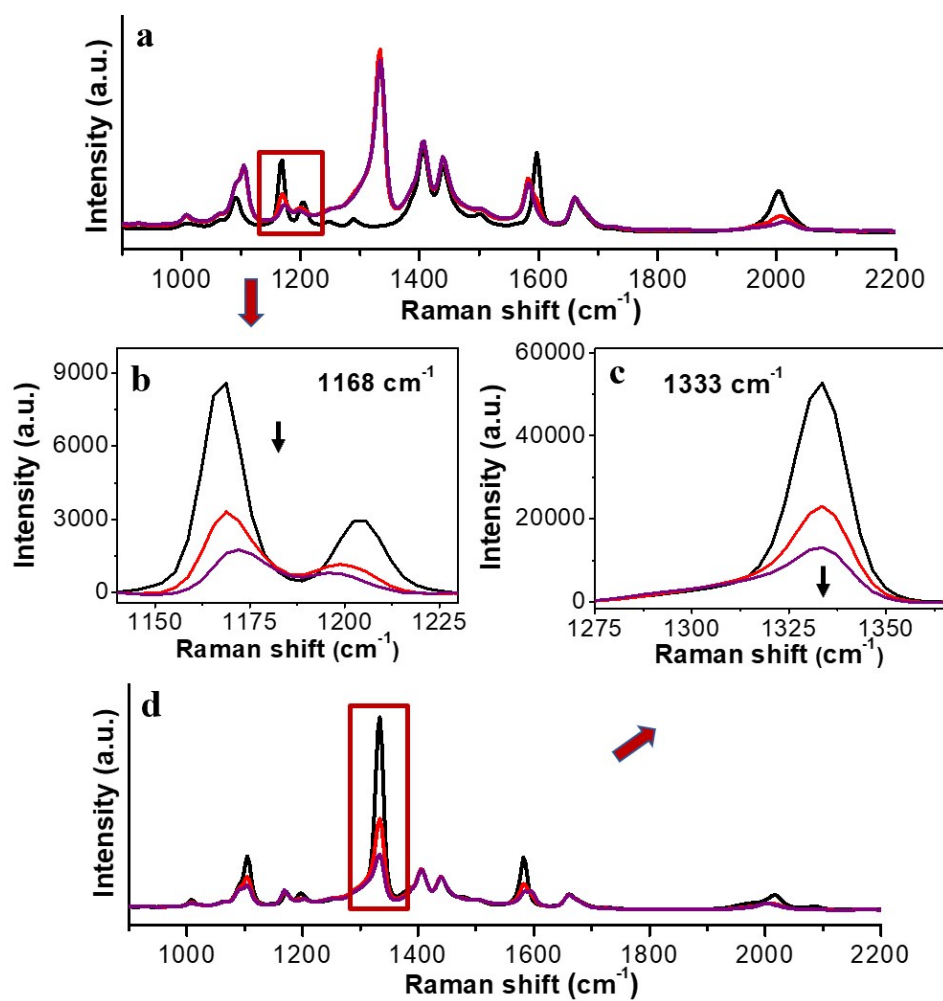


Figure S34. (a) Temporal evolution of the SERS intensity of 8.3 μM 4-AuNPs incubated with 8.2 μM (red) and 82 μM (purple) 3 in DMF. (b) Expansion of the framed region in a. (c) Expansion of the framed region in d. (d) Temporal evolution of the SERS intensity of 8.3 μM 3-AuNPs incubated with 8.2 μM (red) and 82 μM (purple) 4 in DMF.

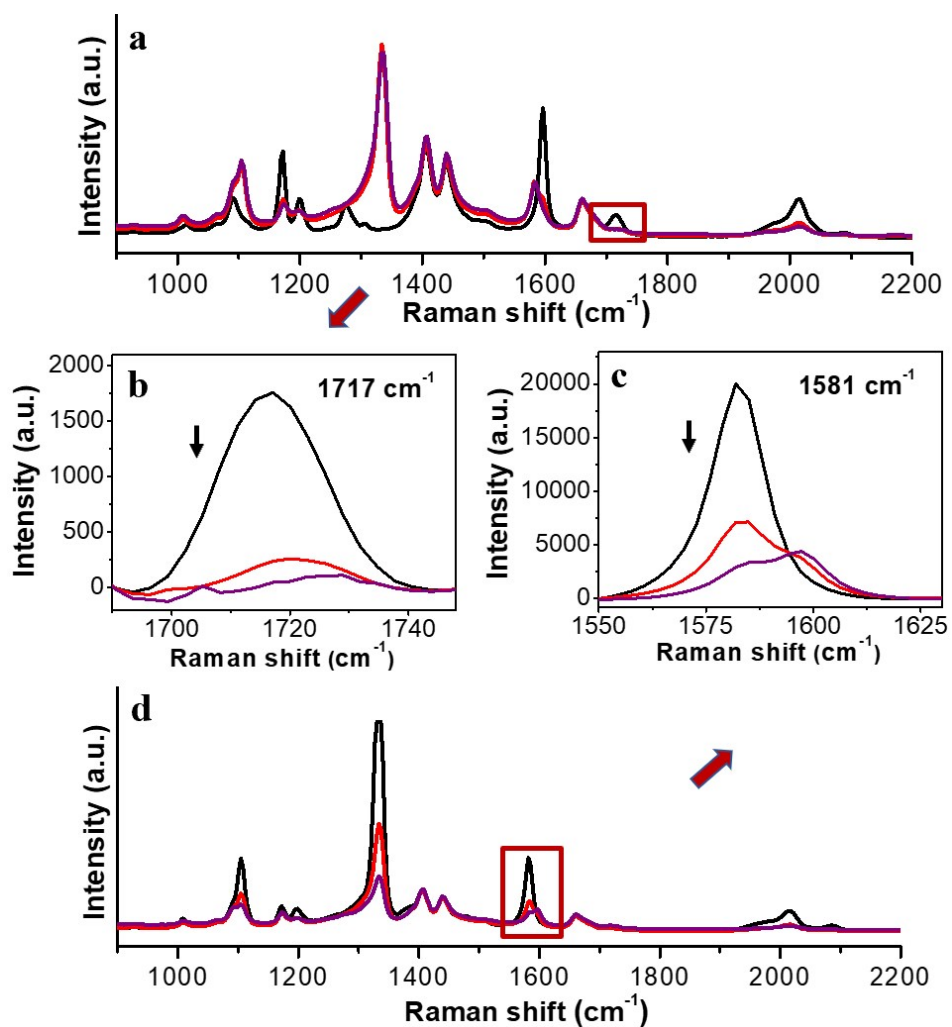


Figure S35. (a) Temporal evolution of the SERS intensity of 8.3 μM 5-AuNPs incubated with 8.2 μM (red) and 82 μM (purple) 3 in DMF. (b) Expansion of the framed region in a. (c) Expansion of the framed region in d. (d) Temporal evolution of the SERS intensity of 8.3 μM 3-AuNPs incubated with 8.2 μM (red) and 82 μM (purple) 5 in DMF.

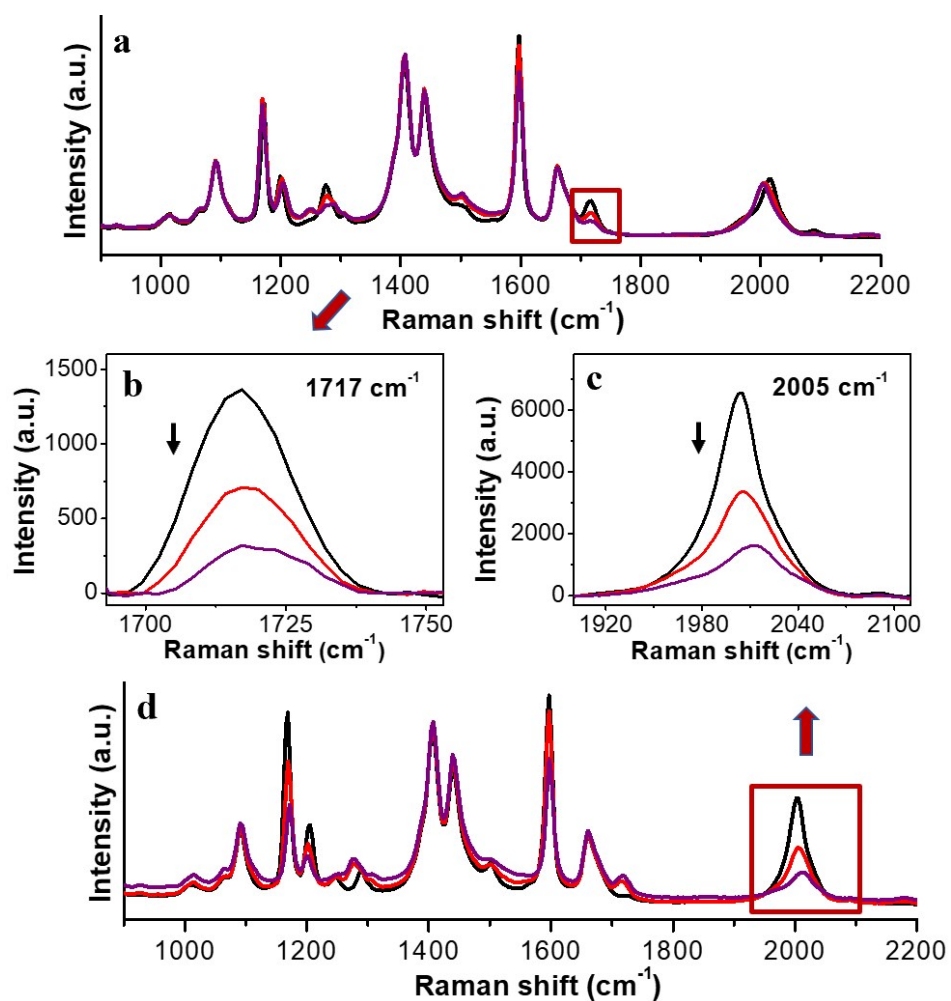


Figure S36. (a) Temporal evolution of the SERS intensity of 8.3 μM 5-AuNPs incubated with 8.2 μM (red) and 82 μM (purple) 4 in DMF. (b) Expansion of the framed region in a. (c) Expansion of the framed region in d. (d) Temporal evolution of the SERS intensity of 8.3 μM 4-AuNPs incubated with 8.2 μM (red) and 82 μM (purple) 5 in DMF.

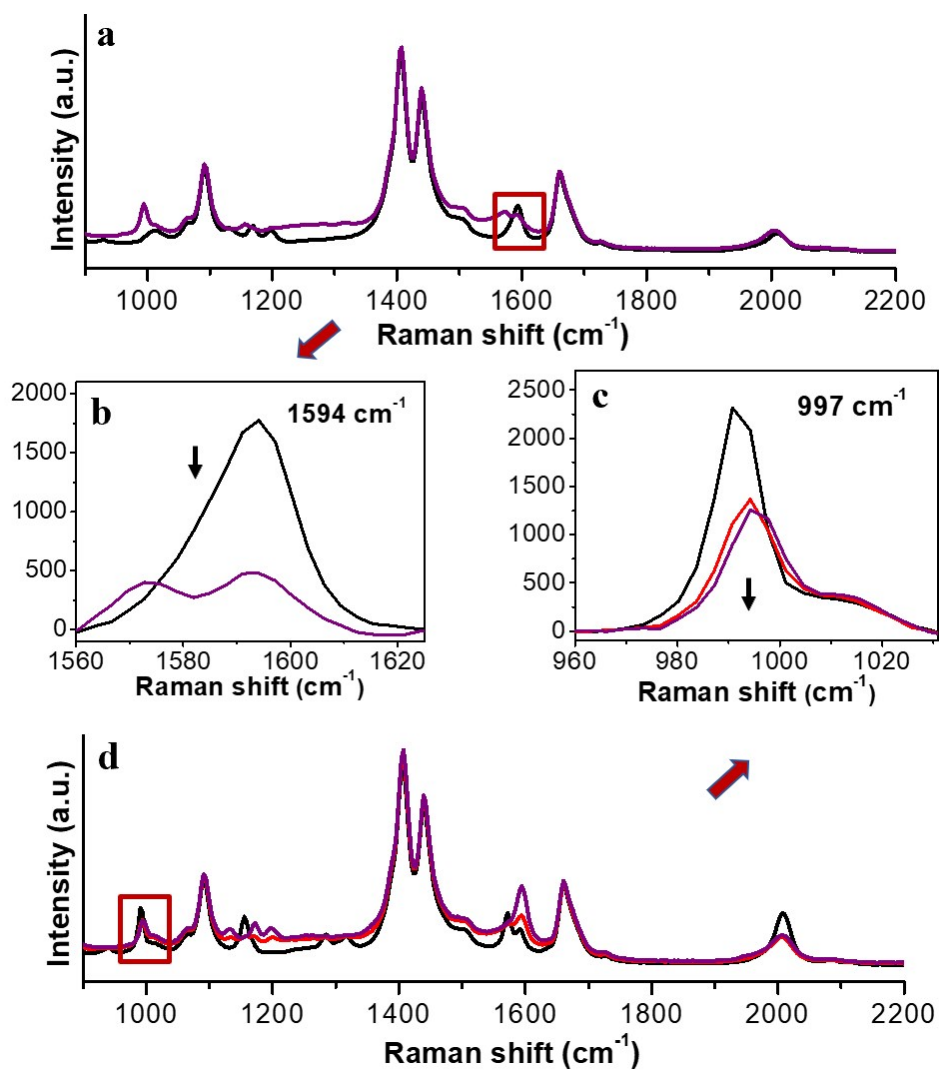


Figure S37. (a) Temporal evolution of the SERS intensity of 8.3 μM 7-AuNPs incubated with 8.2 μM 6 in DMF. (b) Expansion of the framed region in a. (c) Expansion of the framed region in d. (c) Temporal evolution of the SERS intensity of 8.3 μM 6-AuNPs incubated with 8.2 μM (red) and 82 μM (purple) 7 in DMF.

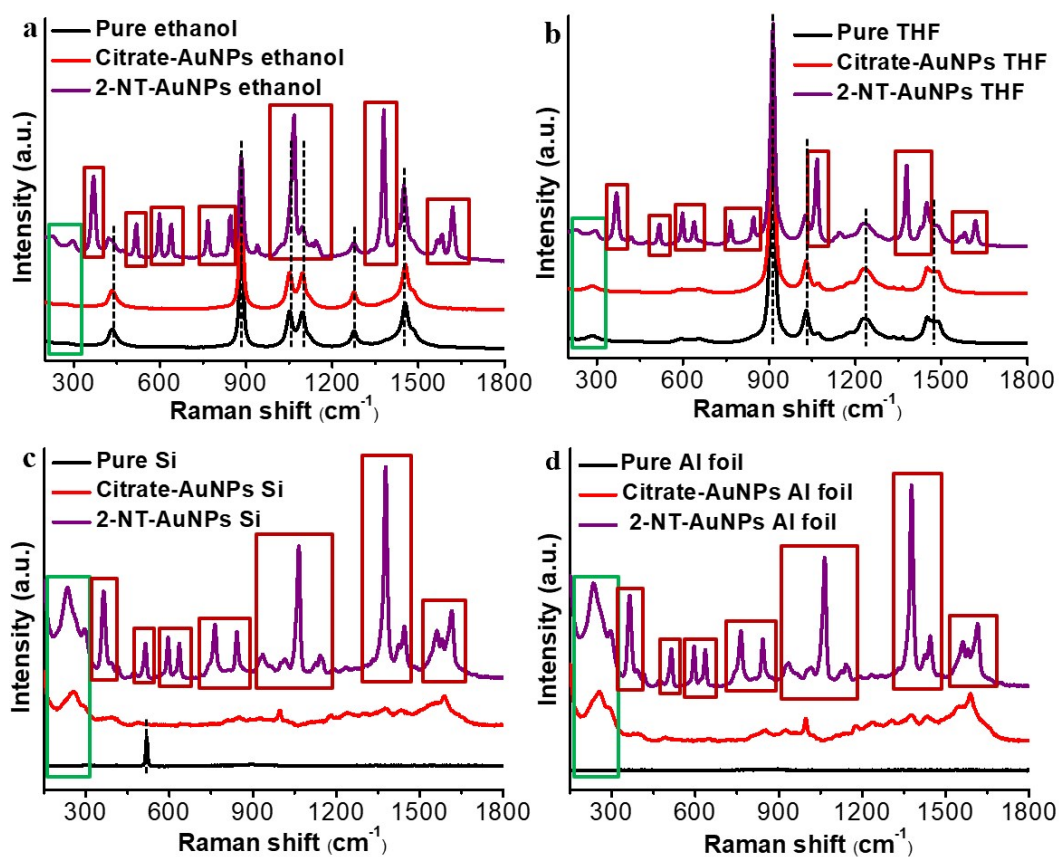


Figure S38. (a) Raman spectra of pure ethanol (black); SERS intensity of 60 nm citrate-AuNPs (red), 2-NT-AuNPs (purple) in ethanol. (b) Raman spectra of pure THF (black); SERS intensity of 60 nm citrate-AuNPs (red), 2-NT-AuNPs (purple) in THF. (c) Raman spectra of pure Si (black); SERS intensity of 60 nm citrate-AuNPs (red), 2-NT-AuNPs (purple) on Si. (d) Raman spectra of pure Al foil (black); SERS intensity of 60 nm citrate-AuNPs (red), 2-NT-AuNPs (purple) on Al foil.

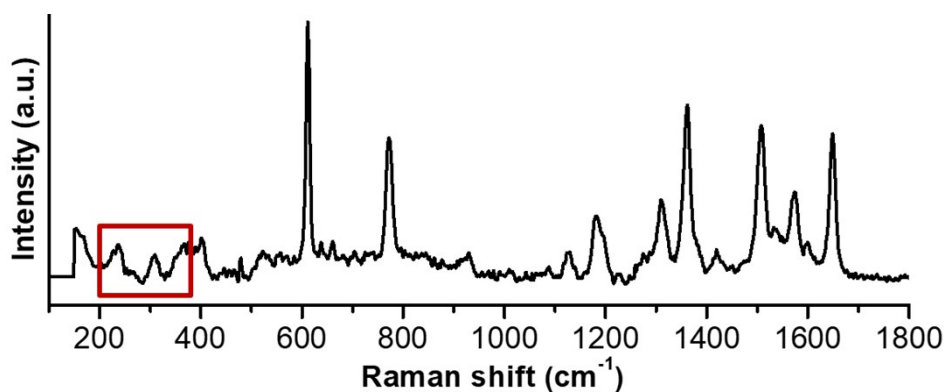


Figure S39. Raman spectra of pure 2-NT powder.

Table S1. Phenynyl ligands (1-7) mutual exchange PhA.

Ligand exchange	Raman shift (cm ⁻¹)	Before	After	Degree
1 ex. PhA (1:1)	997	5461	1428	74%
PhA ex. 1 (1:1)	1985	25131	20215	20%
PhA ex. 1 (10:1)	1985	25131	15566	38%
2 ex. PhA (1:1)	997	5482	3000	45%
PhA ex. 2 (1:1)	1597	13032	10365	20%
PhA ex. 2 (10:1)	1597	13032	7608	42%
3 ex. PhA (1:1)	997	5572	0	100%
PhA ex. 3 (1:1)	1333	43171	12250	72%
PhA ex. 3 (10:1)	1333	43171	12250	72%
4 ex. PhA (1:1)	997	5876	2605	56%
PhA ex. 4 (1:1)	1165	6617	5142	22%
PhA ex. 4 (10:1)	1165	6617	3790	43%
5 ex. PhA (1:1)	997	5489	2030	63%
PhA ex. 5 (1:1)	1274	1583	976	38%
PhA ex. 5 (10:1)	1274	1583	431	73%
6 ex. PhA (1:1)	1588	6263	1812	71%
PhA ex. 6 (1:1)	1155	1307	0	100%
7 ex. PhA (1:1)	1588	6526	5626	14%
PhA ex. 7 (1:1)	1594	990	0	100%

Table S2. Phenynyl ligands (1-7) mutual exchange each other.

Ligand exchange	Raman shift (cm ⁻¹)	Before	After	Degree
1 ex. 2 (1:1)	1284	5937	2510	58%
1 ex. 2 (10:1)	1284	5937	1118	81%
2 ex. 1 (10:1)	1988	31532	17364	45%
1 ex. 3 (1:1)	1333	54670	17560	68%
1 ex. 3 (10:1)	1333	54670	7829	86%
3 ex. 1 (1:1)	1988	24025	23034	4%
3 ex. 1 (10:1)	1988	24025	11162	54%
1 ex. 4 (1:1)	1288	1181	221	81%
1 ex. 4 (10:1)	1288	1181	28	98%
4 ex. 1 (1:1)	1988	32062	30302	5%
4 ex. 1 (10:1)	1988	32062	16670	48%
2 ex. 3 (1:1)	1333	43121	21544	50%
2 ex. 3 (10:1)	1333	43121	13140	70%
3 ex. 2 (1:1)	1178	7729	4589	41%
3 ex. 2 (10:1)	1178	7729	2504	68%
2 ex. 4 (1:1)	1205	3650	1960	46%
2 ex. 4 (10:1)	1205	3650	1201	67%
4 ex. 2 (1:1)	1284	6000	4605	23%
4 ex. 2 (10:1)	1284	6000	2466	59%
3 ex. 4 (1:1)	1168	8319	3311	60%
3 ex. 4 (10:1)	1168	8319	1782	79%
4 ex. 3 (1:1)	1333	52724	23049	56%
4 ex. 3 (10:1)	1333	52724	13123	75%
3 ex. 5 (1:1)	1717	1760	240	86%
3 ex. 5 (10:1)	1717	1760	48	97%
5 ex. 3 (1:1)	1581	20015	7109	64%
5 ex. 3 (10:1)	1581	20015	4393	78%
4 ex. 5 (1:1)	1717	1364	708	48%
4 ex. 5 (10:1)	1717	1364	320	77%
5 ex. 4 (1:1)	2005	6556	3377	48%
5 ex. 4 (10:1)	2005	6556	1631	75%
6 ex. 7 (1:1)	1594	1774	0	100%
7 ex. 6 (1:1)	997	2201	1369	38%
7 ex. 6 (10:1)	997	2201	1211	45%